^{121}Sb Mössbauer Spectra of Hypervalent Complexes Having an Antimony-transition Metal Bond and Partial Quadrupole Coupling Constants

Masashi Takahashi, Atsushi Ishiguro[†], Masaki Maeda, Masuo Takeda, Koichiro Toyota[a], Yohsuke Yamamoto[a], and Kin-ya Akiba[a,b]

Department of Chemistry, Faculty of Science, Toho University,
Miyama, Funabashi, Chiba 274-8510, Japan
[a] Department of Chemistry, Graduate School of Science, Hiroshima University,
Kagamiyama, Higashi-Hiroshima 739-8526, Japan
[b] Advanced Research Center for Science and Engineering, Waseda University,
3-4-1 Ohkubo, Shinjuku-ku, Tokyo 169-8555, Japan
[†] Present address: Department of Material Science, Graduate School of Science and Engineering,
Saitama University, Urawa, Saitama 338-8570, Japan; and
The Institute of Physical and Chemical Research (RIKEN), Wako Saitama 384-0198, Japan

Reprint requests to Prof. M. T.; E-mail: takahasi@chem.sci.toho-u.ac.jp

Z. Naturforsch. **57 a,** 631–639 (2002); received February 26, 2002

Presented at the XVIth International Symposium on Nuclear Quadrupole Interactions, Hiroshima, Japan, September 9-14, 2001.

Antimony-121 Mössbauer spectra for hypervalent pentacoordinate antimony compounds having Sb-transition metal bond [$Rf_2SbMCp(CO)_n$ {RfH = *o*-$C_6H_4C(CF_3)_2OH^-$, M = Fe, Ru, Cr, Mo, W}, $Rf_2SbFeCp(CO)PPh_3$, $Rf_2SbFeCp(dppe)$] and closely related compounds Rf_2SbTol (Tol = *p*-$CH_3C_6H_4$), Rf_2SbX (X = Cl, Br) are described. The strong σ-donor power of the metal fragments is demonstrated by the Mössbauer parameters. The σ-donor power decreases in the order $FeCp(dppe) > FeCp(CO)PPh_3 > FeCp(CO)_2 > RuCp(CO)_2 > CrCp(CO)_3 > MoCp(CO)_3 > WCp(CO)_3 \gg$ Tol. The essential trends in the molecular structure and the Berry pseudorotation are interpreted by this order. In addition, the e^2qQ values for 32 hypervalent antimony compounds are successfully calculated using the additivity model for the e^2qQ value. A unique electronic feature for Rf_2SbX is clarified through the calculation

Key words: ^{121}Sb Mössbauer Spectra; Hypervalent Compound; Organometallic Ligand; Berry Pseudorotation.

1. Introduction

The very low energy barrier for the Berry pseudorotation of pentacoordinate compounds is well known [1, 2]. For example the energy barrier for PF_5 is reported to be only (16 $\pm$ 2) kJ mol^{-1} (ab initio calculation) [3] and 12.7 - 16.4 kJ mol^{-1} (experimental values) [4 - 6]. Recently we have shown that the barrier can be risen by introducing a bidentate ligand such as the so-called Martin ligand {RfH = *o*-$C_6H_4C(CF_3)_2OH^-$}. The chirality of the phosphorane Rf_2P^*H is held even at room temperature [7, 8]. The pseudorotational barrier depends, however, strongly on the monodentate ligand (L) in the equatorial position even in Rf_2M^*L (M = group 15 element). For example, the configuration of Rf_2Sb^*X (X = halogen) is readily scrambled since the electronegative X has high apicophilicity and stabilizes the intermediate of the pseudorotation [9]. In this respect stiborane with organometallic fragment is quite interesting because it has an electron-donating ability. A series of stiboranes, having the organometallic fragment such as $MCp(CO)_n$ (Cp = cyclopentadienyl anion; M = Fe, Ru, n = 2; M = Cr, Mo, W, n = 3) in the equatorial position, are synthesized and well specified [10 - 13]. Large values for the pseudorotational barriers (126 - 139 kJ mol^{-1}) are obtained by the isomerization reaction and discussed in connection with

0932–0784 / 02 / 0600–0631 $ 06.00

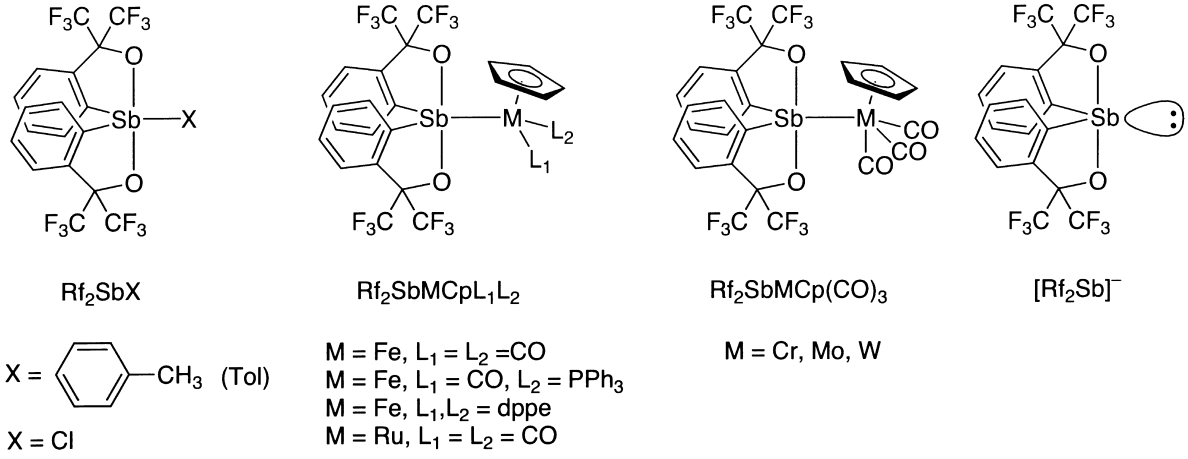

Structural Schemes.

equatophilities of the organometallic fragments. The equatophilicity is thought to result essentially from the electron-donating ability of the organometallic fragment. This work is carried out to obtain direct evidence for the electron-donation of the organometallic fragment using ^{121}Sb Mössbauer spectroscopy.

^{121}Sb Mössbauer spectroscopy has been demonstrated to be a powerful tool for such a purpose. There are some advantages of ^{121}Sb Mössbauer spectroscopy: (i) The isomer shift is very sensitive to small changes in the s electron density since the change in the nuclear radius during the Mössbauer transition ($|\Delta R|/R$) for ^{121}Sb is the largest among the Mössbauer nuclides, (ii) the sign of the electric field gradient is easily determined from the absorption shape since the Mössbauer transition is between I_g = 5/2 and I_e = 7/2, and thus the symmetry of the electron distribution is readily known. We have studied the electronic states of the hypervalent organoantimony compounds [14 - 17] and transition metal carbonyl compounds with M-Sb bond(s) [18, 19].

In this paper the Mössbauer spectra for $Rf_2SbMCp(CO)_n$ (M = Fe, Ru, Cr, Mo, W), $Rf_2SbFeCp(CO)PPh_3$, $Rf_2SbFeCp(dppe)$, Rf_2SbTol, Rf_2SbX (X = Cl, Br) are described. The numbers of electrons donated from the equatorial ligand are derived from the Mössbauer parameters and the results are compared with the molecular structures and the pseudorotational barriers. In addition, the e^2qQ values for the hypervalent antimony compounds are discussed using the additivity model for the e^2qQ-value. Thus the electronic features of Rf_2SbX are clarified.

2. Experimental

All the compounds used in this work were synthesized by the published procedures [10 - 13].

Antimony-121 Mössbauer spectra were measured with an Austin Science S-600 Mössbauer spectrometer using a $Ca^{121m}SnO_3$ source (16 MBq). Both the sample containing 15 mgSb cm^{-2} and the source were kept at 20 K in a cryostat equipped with a closed-cycle refrigerator. The Doppler velocity was measured with an Austin Science LA-9 laser interferometer and calibrated by measuring the ^{57}Fe Mössbauer spectrum of an α-iron foil at 20 K. The ^{121}Sb Mössbauer spectra were computer- fitted to quadrupole-split twelve-lines using a transmission-integral method [20] on a personal computer. The values of the isomer shift (δ) are given relative to InSb at 20 K.

Iron-57 Mössbauer spectra were obtained using a Mössbauer driving system from Wissel GmbH, consisting of MDU-120, DFG-1200 and MVT-1000. The samples containing 6 mgFe cm^{-2} were kept at 80 K and room temperature in a CF1104 continuous gas flow cryostat from Oxford Instruments. The ^{57}Co(Rh)

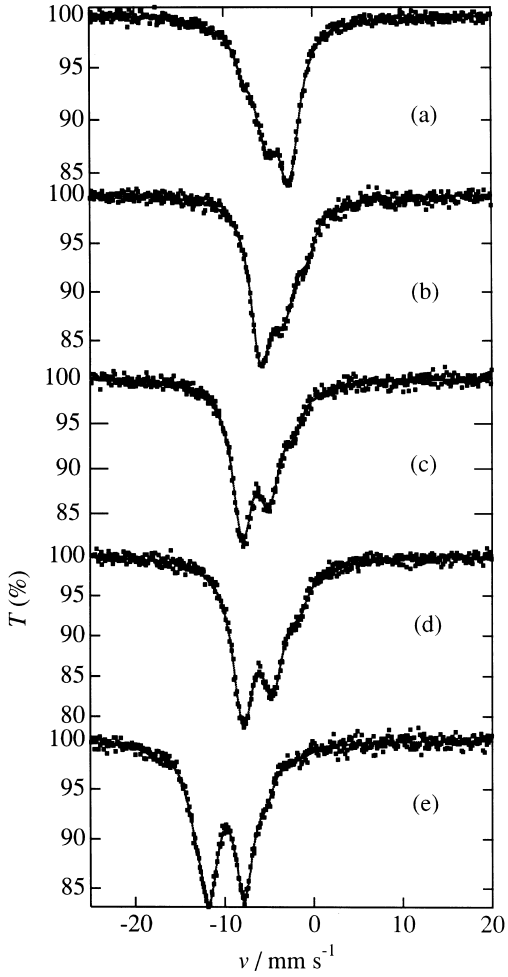

Fig. 1. ^{121}Sb Mössbauer spectra at 20 K for hypervalent antimony compounds, Rf_2SbX. (a) X = Cl, (b) X = Tol, (c) X = $CrCp(CO)_3$, (d) X = $FeCp(CO)_2$, (e) X = Et_4N.

source was kept at room temperature. The spectra were computer-fitted to Lorentzian lines, and the values of the isomer shift (δ_{Fe}) are referred to α-iron at room temperature.

3. Results and Discussion

3.1. σ-donor Power of the Metal Fragments Deduced from ^{121}Sb Mössbauer Parameters

Some typical Mössbauer spectra are shown in Fig. 1, and the Mössbauer parameters are summarized in Table 1. Each compound other than Rf_2SbX (X = Cl, Br) has a large negative quadrupole coupling constant (e^2qQ). The negative e^2qQ indicates the positive V_{zz}, the principal component of the electric field gradient (EFG), since the sign of eQ for ^{121}Sb is negative, and this means that the principal z axis is the apical bond direction of trigonal bipyramidal (tbp) structure, i. e., along the O-Sb-O direction. This positive V_{zz} is the common feature for the organoantimony(V) compound adopting the tbp structure since the electrons in the apical bonds are withdrawn to the ligands. Hence the positive e^2qQ values for Rf_2SbCl and Rf_2SbBr were unexpected because the tbp structure with a Cl atom in the equatorial plane is definitely shown for Rf_2SbCl by the X-ray determination [9]. The problem was, however, solved by choosing the principal axes in a different direction as is discussed later.

Table 1. ^{121}Sb Mössbauer parameters at 20 K, and ΔN_s, ΔN_p and ΔN_{eq} for hypervalent antimony compounds having an antimony-transition metal bond.

Compound Rf_2SbX, X =	δ[a] mms^{-1}	e^2qQ mms^{-1}	η mms^{-1}	Γ_{exp} mms^{-1}	ΔN_s[b]	ΔN_p[b]	ΔN_{eq}[b]
Tol	4.16	–18.3	0.15	2.50			
$FeCp(CO)_2$	2.46	–21.3	0.34	2.37	0.12	0.23	0.35
$FeCp(CO)PPh_3$	2.07	–23.6	0.37	2.64	0.15	0.41	0.56
FeCp(dppe)	1.18	–23.6	0.38	2.28	0.21	0.41	0.62
$RuCp(CO)_2$	2.71	–21.2	0.33	2.27	0.10	0.22	0.33
$CrCp(CO)_3$	2.35	–20	0.32	2.45	0.12	0.13	0.25
$MoCp(CO)_3$	2.48	–19.8	0.44	2.19	0.12	0.12	0.23
$WCp(CO)_3$	2.67	–19.7	0.49	2.31	0.10	0.11	0.21
(Et_4N)	–1.37	–24.9	0.84	2.52	0.38	0.51	0.89
Cl	4.35	+17.8	0.24	2.55			
Br	4.16	+17.3	0.17	2.50			

[a] Relative to InSb at 20 K, [b] Values are given relative to Rf_2SbTol.

Both the isomer shift (δ) and e^2qQ of the metal ligand complexes are intermediate of those for $[Rf_2Sb]^-$ and Rf_2SbTol (Tol = p-$CH_3C_6H_4$), as shown in Figure 2. This means that the electronic states of Rf_2SbX are similar and vary continuously when the equatorial ligand is changed from Tol to metal ligands and even the lone pair. In this paper the lone pair is considered as a kind of ligand. It is interesting that the classification by the oxidation number is meaningless for these compounds though the oxidation numbers are calculated to be +III for $[Rf_2Sb]^-$ and +V for Rf_2SbTol and the metal ligand compounds.

The increase in e^2qQ for the metal ligand compounds compared with that for Rf_2SbTol indicates an increase in p electron imbalance. This is interpreted by σ-donation from the metal fragment to the p_x and p_y orbital of Sb. π-donation of a p_z electron in the

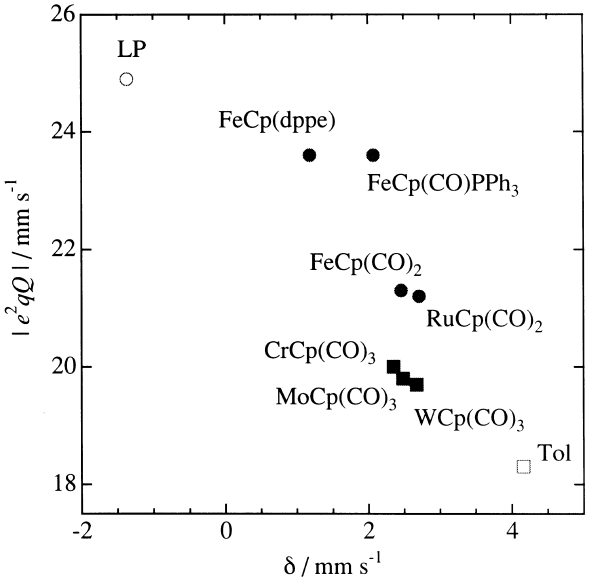

Fig. 2. Plot of $|e^2qQ|$ against δ for Rf_2SbX. The meaning of X is given in the figure.

apical Sb-O bond into the transition metal d orbital may be an alternative interpretation. The Sb←M σ-donation, however, would be plausible because the metal fragments, isolobal to Tol, are known to act as good electron-donors. The X-ray determinations for the metal ligand compounds [10 - 14] support the σ-donation mechanism; The apical Sb-O lengths of these compounds are longer, and the apical O-Sb-O angles are smaller, than those of Rf_2SbTol [21], indicating that the metal fragments are electron-donating. It is noteworthy that the π-back donation of the metal fragment into the axial antibonding MO of Sb, which is found in the hypervalent phosphoranes with the iron fragment [22], is not important because such π-back donation should cause a decrease in the e^2qQ value. The δ values, showing the electron density at the Sb nucleus, reflect the Sb 5s electron density directly and the Sb 5p density indirectly through the shielding effect of the p electrons. These effects operate oppositely. Since δ decreases as $|e^2qQ|$ increases, the change in δ reflects the direct change in s electron density.

We can estimate the change in valence electron populations of the Sb atom using the Mössbauer parameters for Rf_2SbTol as a reference according to the Parish's method [23]. The Mössbauer parameters are closely related to the electron configuration of the Mössbauer atom by [23, 24]

$$U_p = -e^2qQ/(e^2qQ)_0 = -N_z + \frac{1}{2}(N_x + N_y), \quad (1)$$

$$\delta = aN_s + bN_p, \quad (2)$$

where U_p is the p electron imbalance, $(e^2qQ)_0$ is the electric field gradient for $U_p = 1$, $N_{s,x,y,z}$ are the populations of 5s and $5p_{x,y,z}$ orbitals, respectively, and a and b are proportionality constants. Expecting a negligible change in the apical bond character (namely $\Delta N_z = 0$), we can estimate the change in p electron populations in the equatorial plane by

$$\Delta N_p = \Delta N_x + \Delta N_y = -2\Delta(e^2qQ)/(e^2qQ)_0 \quad (3)$$

$$= -2[e^2qQ - (e^2qQ)_{Rf_2SbTol}]/(e^2qQ)_0,$$

where for $(e^2qQ)_0$ the value 26 mm s^1 is proposed by Parish [23]. Once the ΔN_p value is obtained, we can evaluate the change in s electron population ΔN_s by

$$\Delta\delta = \delta - \delta_{Rf_2SbTol} = a\Delta N_s + b\Delta N_p, \quad (4)$$

where a = –15.0 and b = 0.80 mm s^{-1} [23]. The estimated ΔN_s and ΔN_p and ΔN_{eq} (= ΔN_s + ΔN_p) values are also listed in Table 1 [25].

The σ-donor power of the metal fragments decrease in the order $FeCp(CO)_2 > RuCp(CO)_2 \gg CrCp(CO)_3 > MoCp(CO)_3 > WCp(CO)_3$. Obviously the donor power of group 8 metals is larger than that of group 6 metal. This agrees with the basicities of the metal fragments viewed by the reactivity with alkyl halides [26], but the differences within the same group are small and the order of the σ donor power for the group 6 metals is contrary to the reported order. In contrast, the ΔN_{eq} values increase enormously on substituting the carbonyl ligand in the iron fragment by phosphine ligands. The strong σ-donor power is directly reflected in the $FeCp(CO)PPh_3$ and FeCp(dppe) complex, suggesting that the electron from the phosphine ligand is transferred to the antimony atom. The ^{57}Fe Mössbauer parameters for these compounds (Table 2) support this. The isomer shift (δ_{Fe}) increases in the order $FeCp(CO)_2 < FeCp(CO)PPh_3 <$ FeCp(dppe). This suggests that the s electron density decreases in that order, suggesting an increased σ-donation of the metal fragments. The quadrupole splitting (ΔE_q) changes only slightly in spite of the substitution of

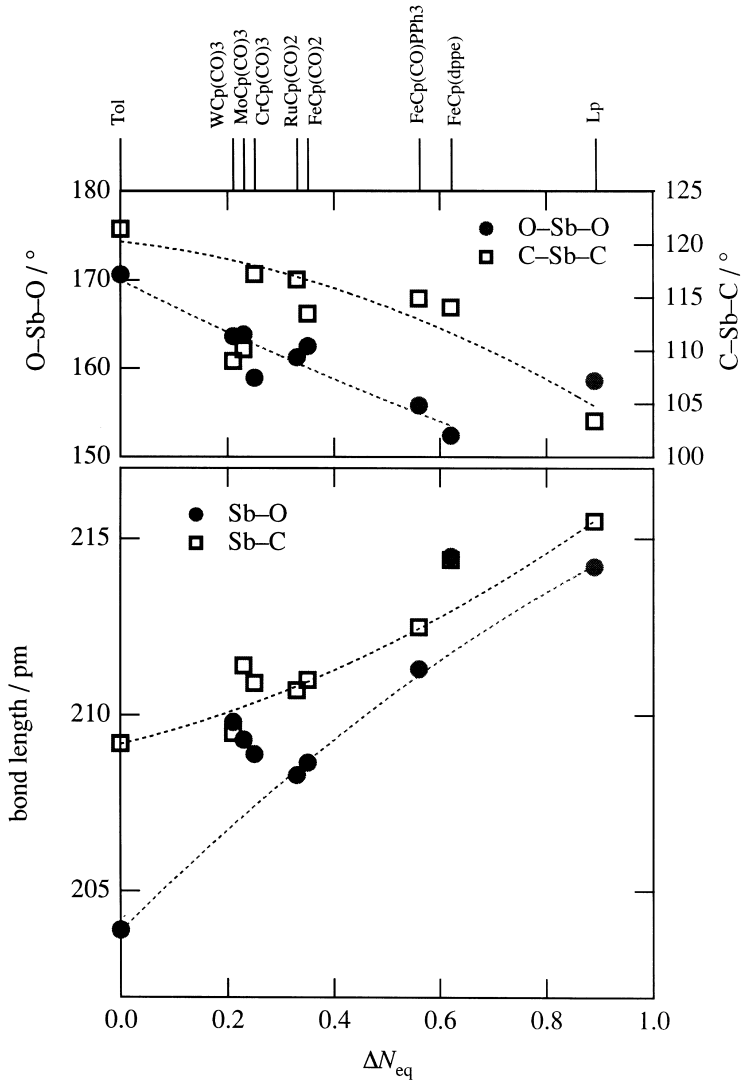

Fig. 3. Dependence of the molecular geometry on the increase of the electron density in the equatorial plane (ΔN_{eq}).

Table 2. ^{57}Fe Mössbauer parameters for hypervalent antimony compounds having an antimony-iron bond.

Compound	Temp.	$\frac{\delta_{Fe}}{mm\,s^{-1}}$	$\frac{\Delta E_q}{mm\,s^{-1}}$
$Rf_2SbFeCp(CO)_2$	rt	0.06	1.78
	80 K	0.14	1.80
$Rf_2SbFeCp(CO)PPh_3$	rt	0.18	1.85
	80 K	0.23	1.86
$Rf_2SbFeCp(dppe)$	rt	0.29	1.81
	80 K	0.36	1.79

electron-attracting carbonyl to the electron-donating phosphine ligand.

A close examination of the change in the valence electron populations implies that σ donation to the Sb 5p orbital is dominant for most of the metal fragments, and σ donation to the Sb 5s orbital (ΔN_s = 0.10 - 0.12) does not vary significantly among the metal fragments, while the substitutions of the carbonyl ligand in the iron fragment to the phosphine ligands cause much increase in ΔN_s (ΔN_s = 0.12, 0.15, 0.21 for $Rf_2SbFeCp(CO)_2$, $Rf_2SbFeCp(CO)PPh_3$ and $Rf_2SbFeCp(dppe)$, respectively).

3.2. Relation between σ Donor Power and Molecular Structure

Some geometrical parameters established by X-ray determinations are plotted against the ΔN_{eq} values in

Figure 3. Clearly the apical Sb-O and equatorial Sb-C bond lengths are elongated and the apical O-Sb-O and equatorial C-Sb-C bond angles are reduced according to the increase of the electron densities in the equatorial plane caused by the σ donation of the metal fragments. This evidently indicates that the equatorial accumulation of electrons results in a distortion of the ideal tbp structure. The distortion is essentially due to the electron-electron repulsion origining from the Pauli principle, as is emphasized in the valence-shell electron pair repulsion theory (VSEPR) [27].

In the plot of Fig. 3, the positions for FeCp(dppe) and the group 6 metal fragments deviate from the smooth line. The FeCp(dppe) fragment has a large dppe ligand having four phenyl groups and the $MCp(CO)_3$ fragments have one extra CO ligand compared with the iron fragment $FeCp(CO)_2$. Thus the deviation from the tbp structure would be enhanced due to the bulkiness of those fragments. The facts that the bond lengths for these fragments are deviated to the elongated direction and the deviation is larger for heavier metal fragment support this idea.

The equatophilicity is obviously ascribed to the strong σ donation power of the metal fragments. The Mössbauer spectra give the experimental support for the high equatophilicity for the metal fragments. The pseudorotational barrier for RfRfm*SbFeCp(CO)$_2$ (128, 128 kJ mol^{-1}) is much larger than that for RfRfm*SbTol (118, 117 kJ mol^{-1}), where Rfm denotes *o*-$C_6H_4C(CF_3)(CH_3)O^{2-}$ [28]. This is well explained by the increased equatophilicity for the iron fragment resulting from the strong electron-donating power. The large barriers for RfRfm*SbMoCp(CO)$_3$ and RfRfm*SbMCp(CO)$_2$ (M = Fe, Ru) [12, 13] are also explained by the high equatophilicity. There is, however, a discrepancy between the order of the energy barrier and the σ donor power implied from the Mössbauer spectra. The barrier for pseudorotation increases in the order RfRfm*SbMoCp(CO)$_3$ (131, 133 kJ mol^{-1}) > RfRfm*SbRuCp(CO)$_2$ (128, 127 kJ mol^{-1}) $\geq$ RfRfm*SbFeCp(CO)$_2$ (127, 126 kJ mol^{-1}) [29]. This disagrees with the σ donor power deduced from the Mössbauer parameters. The discrepancy may be ascribed to the steric effect as discussed already . The Mössbauer spectra are related to the electronic state, while the molecular structure and reactivity reflect both the electronic state and steric effect. Hence some discrepancy between them would be inevitable.

3.3. Additive Model for e^2qQ of Organoantimony Compounds

Additive models for EFG have been successfully used for the explanations of ^{119}Sn Mössbauer quadrupole splitting data for organotin compounds [30]. Ruddick et al have applied the model to e^2qQ of ^{121}Sb Mössbauer spectra to give a quantitative explanation of the electronic states of organoatimony(V) compounds [31]. We will extend the model to our hypervalent antimony compounds.

According to the so-called point-charge model, the principal component of the EFG are written as [30, 31]

$$V_{xx} = \sum_{\mathrm{L}} (3\sin^2\theta\cos^2\phi - 1)[\mathrm{L}], \tag{5}$$

$$V_{yy} = \sum_{\mathrm{L}} (3\sin^2\theta\sin^2\phi - 1)[\mathrm{L}], \tag{6}$$

$$V_{zz} = \sum_{\mathrm{L}} (3\cos^2\theta - 1)[\mathrm{L}], \tag{7}$$

where [L] is the partial quadrupole coupling constant of ligand L, and θ and ϕ are the angles in polar coordinates. We will call [L] the partial quadrupole splitting (pqs) parameter, adopting conventional naming, and scale by multiplying $e|Q|$ with V_{zz} for the experimental use. Thus the experimentally obtained e^2qQ and V_{zz} are simply related by

$$e^2qQ = \mathrm{sign}(Q)V_{zz} = -\sum_{\mathrm{L}} (3\cos^2\theta - 1)[\mathrm{L}]. \tag{8}$$

Ruddick et al. have given the pqs parameters for some typical ligands at the apical and equatorial position of tbp, denoted as $[L]^{tba}$ and $[L]^{tbe}$, respectively [29]. Since we cannot obtain the absolute pqs values, they are referred to $[Cl]^{tba}$. The values are summarized in Table 3. Adopting their values, we have calculated several pqs parameters. Although Ruddick et al. have proposed the value of $\pm$0.9 mm s^{-1} for $[Cl]^{tbe}$, we have employed +0.9 mm s^{-1} for our calculations since Bancroft and Platt have suggested a positive value [30].

$[Tol]^{tba}$, $[Ar]^{tba}$, $[I]^{tba}$, $[Tol]^{tbe}$ and $[Ar]^{tbe}$ have been calculated from the e^2qQ values for Tol_3SbCl_2, Ar_3SbCl_2, Ph_3SbI_2, Tol_4SbBr and Ar_5Sb (Ar = *p*-CF_3-C_6H_4). The pqs parameters for the Martin ligand RfH_2 have been estimated on the assumptions: The pqs parameters for the carbon atom of RfH_2, $[C_M]^{tbe}$

Table 3. ^{121}Sb partial quadrupole splitting parameters ([L]) for various ligands in tbp geometry.

Ligand[a]	[L][b] / mm s^{-1}	Source	Ref.
Apical:			
[Ph]^{tba}	–7.2	Ph_4SbCl	[31]
[OH]^{tba}	–0.3	Ph_4SbOH	[31]
[Br]^{tba}	–0.2	Ph_3SbBr_2	[31]
[Cl]^{tba}	0	reference	[31]
[F]^{tba}	+0.3	Ph_3SbF_2	[31]
[Tol]^{tba}	–7.0	Tol_4SbBr	this work
[Ar]^{tba}	–3.7	Ar_5Sb	this work
[I]^{tba}	–0.9	Ph_3SbI_2	this work
[O_M]^{tba}	–0.3	postulated	this work
Equatorial:			
[CH_3]^{tbe}	–8.0	$(CH_3)_3SbCl_2$	[31]
[Ph]^{tbe}	–6.9	Ph_3SbCl_2	[31]
[Tol]^{tbe}	–6.6	Tol_3SbCl_2	this work
[Ar]^{tbe}	–6.5	Ar_3SbCl_2	this work
[C_M]^{tbe}	–6.6	R_3SbCl_2	this work
[Br]^{tbe}	+0.2	Rf_2SbBr	this work
[Cl]^{tbe}	+0.9[c]	$SbCl_5$	this work, [31]

[a] tba = trigonal bipyramidal apical, tbe = trigonal bipyramidal equatorial. [b] Value tabulated is relative to Cl in equatorial plane, see text. [c] See text.

Table 4. Comparison of observed e^2qQ values with those calculated using partial quadrupole splitting parameters.

Compound	e^2qQ / mm s^{-1}	e^2qQ_{calcd} / mm s^{-1}	Ref.
Ph_3SbCl_2	–20.7	–20.7	[15]
Ph_3SbBr_2	–19.6	–19.9	[15]
Ph_3SbI_2	–17.0	–17.1	[15]
Tol_3SbF_2	–21.5	–21.0	[15]
Tol_3SbCl_2	–19.8	–19.8	[15]
Tol_3SbBr_2	–18.6	–19.0	[15]
Tol_3SbI_2	–15.5	–16.2	[15]
Ar_3SbCl_2	–19.6	–19.5	[15]
Ar_3SbBr_2	–17.7	–18.7	[15]
Ar_3SbI_2	–13.7	–15.9	[15]
Rf_2SbTol	–18.3	–18.6	[14]
$RfSbTol_2F$	–20.2	–19.8	[14]
$RfSbTol_2Cl$	–19.2	–19.2	[14]
$RfSbTol_2Br$	–18.4	–18.8	[14]
$RfSbTol_2I$	–16.6	–17.4	[15]
$RfSbTol_3$	–5.7	–5.2	[15]
Rf_2SbCl	+17.8	+16.8	this work
Rf_2SbBr	+17.3	+17.3	this work
Ph_4SbCl	–6.2	–6.3	[15]
Ph_4SbBr	–7.5	–5.9	[15]
Ph_4SbI	–5.2	–4.5	[15]
Tol_4SbBr	–3.4	–4.0	unpublished
Tol_4SbI	–3.4	–4.0	unpublished
Tol_5Sb	–4.3	–8.2	unpublished
Ar_5Sb	–4.7	–4.7	unpublished

is estimated to be –6.6 mm s^{-1}, which is an average of [Ph]^{tbe}, [Tol]^{tbe} and [Ar]^{tbe}. The pqs parameter for the oxygen atom of RfH, [O_M]^{tba} is assumed to be equal to that of [OH]^{tba}, i. e. [O_M]^{tba} = –0.3 mm s^{-1}. Since the hydroxyl group of RfH_2 is known to behave as an electron-withdrawing group, our assumption would be appropriate. These values are also included in Table 3.

Using the pqs parameters listed in Table 3, the e^2qQ values for 24 pentacoordinate organoantimony(V) compounds are calculated (Table 4). The disagreements between observed and calculated values are within 1.0 mm s^{-1} with the exception of Ar_3SbI_2, Ph_4SbBr and Tol_5Sb. The result is completely satisfactory. The [Ar]^{tbe} value seems to be less reliable since the agreements are somewhat poor for Ar compounds. Notably the agreements for the Martin ligand complexes {Rf_2SbTol, RfSbTolX (X = F, Cl, Br, I) and $RfSbTol_3$} are quite good in spite of the assumed values for [O_M]^{tba} and [C_M]^{tbe}. Thereby we can confirm the validity of the pqs parameters listed in Table 3 and the effectiveness of the additive model for the e^2qQ values.

3.4. Interpretation of the Negative e^2qQ Values of Rf_2SbX

Rf_2SbCl and Rf_2SbBr exceptionally have positive e^2qQ values in spite of the tbp structures. At first an octahedra dimer structure was speculated, but this turned out to be not the case by the X-ray determination [9]. We have noticed that the choice of the principal axes gives a reasonable interpretation in the course of the examination of e^2qQ values using the additive model. Three possibilities for the principal axes of the EFG for the tbp structure are presented in Figure 4. According to choice I, being the usual choice for the tbp structure, V_{zz} for Rf_2SbCl is calculated as

$$\begin{aligned} V_{zz} &= (3\cos^2 0^\circ - 1)[O_M]^{tba} \\ &\quad + (3\cos^2 180^\circ - 1)[O_M]^{tba} \\ &\quad + 2\,(3\cos^2 90^\circ - 1)[C_M]^{tbe} \\ &\quad + (3\cos^2 90^\circ - 1)[Cl]^{tbe} \\ &= 4\,[O_M]^{tba} - 2\,[C_M]^{tbe} - [Cl]^{tbe} \\ &= 11.1 \text{ mm s}^{-1}, \end{aligned}$$

and the calculated e^2qQ value becomes –11.1 mm s^{-1}. This is apparently inconsistent with the observed value (+17.8 mm s^{-1}) because the sign of e^2qQ is opposite and the absolute value is somewhat small.

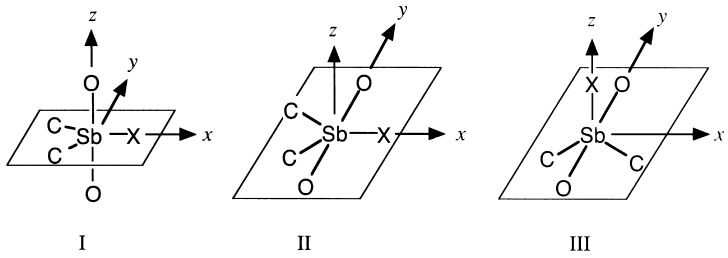

Fig. 4. Possible candidates for the definition of the principal axes of the EFG.

For choice II, taking interchanged apical and equatorial axes, we obtain

$$\begin{aligned} V_{zz} &= (3\cos^2 30^\circ - 1)[\mathrm{C_M}]^{\mathrm{tbe}} \\ &\quad + (3\cos^2 150^\circ - 1)[\mathrm{C_M}]^{\mathrm{tbe}} \\ &\quad + 2\,(3\cos^2 90^\circ - 1)[\mathrm{O_M}]^{\mathrm{tba}} \\ &\quad + (3\cos^2 90^\circ - 1)[\mathrm{Cl}]^{\mathrm{tbe}} \\ &= \tfrac{5}{2}\,[\mathrm{C_M}]^{\mathrm{tbe}} - 2\,[\mathrm{O_M}]^{\mathrm{tba}} - [\mathrm{Cl}]^{\mathrm{tbe}} \\ &= -16.8\ \mathrm{mm\ s^{-1}}, \end{aligned}$$

The calculated e^2qQ value (+16.8 mm s^{-1}) agrees well with the observed one. For choice III, V_{zz} is calculated to be 5.7 mm s^{-1}. Clearly this disagrees with the observation. Hence we conclude that the principal axes for Rf_2SbCl should be taken according to choice II. This choice is reasonable if we think of the electron distribution. The electrons of the Sb atom are withdrawn to two axial O atoms and one equatorial Cl atom, forming the electron deficient ClO_2 plane, while the electron-rich Sb—C bonds are inclined to the z axis. This configuration gives a nearly prolate charge distribution, that is $Vzz < 0$. In most of the pentacoordinate hypervalent antimony compounds the p electrons are withdrawn to two apical electronegative atoms, and as a result the electrons are distributed much more in the equatorial plane than in the apical directions. In this case the charge distribution is oblate and the sign of V_{zz} comes to positive. Thus the electron distribution for Rf_2SbX is distinctive as a pentacoordinate hypervalent compound.

The V_{xx} and V_{yy} components of the EFG for Rf_2SbCl are calculated to be 3.7 and 13.1 mm s^{-1}, respectively, using (5 - 7). Thus the asymmetry parameter η is calculated as

$$\eta = \frac{V_{xx} - V_{yy}}{V_{zz}} = 0.56.$$

Although the calculated value is slightly larger than the observed one (0.24), the difference is acceptable if we take into account that the calculation is based on the ideal tbp structure.

Table 5. Partial quadrupole splitting parameters for organometallic and organic fragments at equatorial position of the trigonal bipyramidal structure.

Ligand	$[L]^{tbe}$ / mm s^{-1}	Ligand	$[L]^{tbe}$ / mm s^{-1}
lone pair	–12.9	FeCp(dppe)	–11.6
$FeCp(CO)PPh_3$	–11.6	$FeCp(CO)_2$	–9.3
$RuCp(CO)_2$	–9.2	CH_3	–8.0
$CrCp(CO)_3$	–8.0	$MoCp(CO)_3$	–7.8
$WCp(CO)_3$	–7.7	Ph	–6.9
C_M	–6.6	Tol	–6.6
Ar	–6.5	Br	+0.2
Cl	+0.9		

We can also calculate the pqs parameters for the metal fragments and the lone pair. The values are listed in Table 5. The pqs parameters for the iron fragments are large and donate much more electrons than the organic ligands such as CH_3, Ph and Tol. Interestingly the pqs parameter for FeCp(dppe) and $FeCp(CO)PPh_3$ are close to that of the lone pair. The σ-donor power of the group 6 fragments is smaller but still donates more electrons to the equtorial plane than Ph and Tol.

In conclusion, the ^{121}Sb Mössbauer spectra indicate the strong σ-donor power of the metal fragments in the pentacoordinate hypervalent antimony compounds having the antimony-group 6 and 8 transition metal bond. The σ-donor power decreases in the order FeCp(dppe) > $FeCp(CO)PPh_3$ > $FeCp(CO)_2$ > $RuCp(CO)_2$ > $CrCp(CO)_3$ > $MoCp(CO)_3$ > $WCp(CO)_3$. The essential trends in the electron distribution and the Berry pseudorotation barrier are interpreted by the above order. Some steric effects for the bulky fragments are also suggested for the molecular structure and the barrier. In addition, the e^2qQ values were successfully calculated for 25 hypervalent compounds using the additive model for the EFG. The different principal z axis of EFG for Rf_2SbCl is demonstrated by the calculation of V_{zz} using the

proposed pqs parameters and this implies its unique electronic feature.

Part of this work was supported by Grants in Aid for Scientific Research (Nos. 06453053 for M. T. 09239103, 09440218, 11166248. 11304044 for Y. Y. and K.-y. A.) from the Ministry of Education Science, Sports, and Culture, Japan.

[1] R. S. Berry, J. Chem. Phys. **32**, 933 (1960).
[2] R. R. Holmes, Pentacoordinated Phosphorus, ACS Monograph Series 175 and 176, American Chemical Society, Washington DC, 1980.
[3] C. J. Marsden, J. Chem. Soc., Chemical Commun. **1984**, 401.
[4] L. S. Bernstein, S. Abramowitz, and I. W. Levin, J. Chem. Phys. **64**, 3228 (1976).
[5] V. P. Spiridonov, A. A. Ishchenko, and L. S. Ivaskevich, J. Mol. Struct. **72**, 153 (1981).
[6] L. S. Bernstein, J. J. Kim, K. S. Pitzer, S. Abramowitz, and I. W. Levin, J. Chem. Phys. **62**, 3671 (1975).
[7] S. Kojima, K. Kajiyama, and K.-y. Akiba, Bull. Chem. Soc. Japan **68**, 1785 (1995).
[8] S. Kojima, K. Kajiyama, and K.-y. Akiba, Tetrahedron Lett. **35**, 7037 (1994).
[9] S. Kojima, R. Takagi, H. Nakata, Y. Yamamoto, and K.-y. Akiba, Chem. Lett. **1995**, 857.
[10] Y. Yamamoto, M. Okazaki, Y. Wakisaka, and K.-y. Akiba, Organometallics **14**, 3364 (1995).
[11] K. Toyota, Y. Yamamoto, and K.-y. Akiba, Chem. Lett. **1999**, 783.
[12] K. Toyota, Y. Wakisaka, Y. Yamamoto, and K.-y. Akiba, Organometallics **19**, 5122 (2000).
[13] K. Toyota, Y. Yamamoto, and K.-y. Akiba, Organometallics **19**, 5134 (2000).
[14] M. Takeda, M. Takahashi, Y. Yanagida, S. Kojima, and K.-y. Akiba, Chem. Lett. **1993**, 2037.
[15] M. Takeda, M. Takahashi, Y. Yanagida, S. Kojima, K.-y. Akiba, and Y. Ito, Hyperfine Interact. **84**, 439 (1994).
[16] M. Takeda, M. Takahashi, Y. Yanagida, S. Kojima, and K.-y. Akiba, Conf. Proc. - Ital. Phys. Soc. **50**, 107 (1996).
[17] M. Yanaga, K. Endo, T. Shimizu, H. Nakahara, M. Takahashi, and M. Takeda, Hyperfine Interact. **90**, 499 (1994).
[18] M. Maeda, M. Takahashi, and M. Takeda, J. Radioanal. Nucl. Chem. **239**, 233 (1999).
[19] A. Ishiguro, M. Takahashi, and M. Takeda, J. Organomet. Chem. **611**, 558 (2000).
[20] G. K. Shenoy, J. M. Friedt, H. Maletta, and S. L. Ruby in I. J. Gruverman, C. W. Seidel, and D. K. Dieterly (eds), Mössbauer Effect Methodology, Vol. 9, Plenum, New York 1975.
[21] S. Kojima, Y. Doi, M. Okuda, and K.-y. Akiba, Organometallics **14**, 1928 (1995).
[22] K. Kubo, H. Nakazawa, and K. Miyoshi, Organometallics **17**, 3522 (1998).
[23] R. V. Parish, Coord. Chem. Rev. **42**, 1 (1982).
[24] R. V. Parish, Mössbauer Eff. Ref. Data J. **5**, 49 (1982).
[25] The accuracy of the Mössbauer parameter is required for this calculation. We have confirmed that our e^2qQ and η values agree almost perfectly with the values from nuclear quadrupole resonance; Y. Kajitani, M. Takahashi and M. Takeda, Int. J. Inorg. Mat. **3**, 337 (2001).
[26] R. E. Dessy, R. L. Pohl, and R. B. King, J. Am. Chem. Soc. **88**, 5121 (1966).
[27] R. J. Gillespie and E. A. Robinson, Angew. Chem. Int. Ed. Engl. **35**, 495 (1996).
[28] These values are determined in *o*-dichlorobenzene at 413 K. See [12]. The value for Rf_2SbTol measured in the same solvent at 298 K is 114 kJ mol^{-1} and is very close to those of RfRfm*SbTol but the values for $Rf_2SbFeCp(CO)_2$ can not be determined due to decomposition. See [10].
[29] These values are measured in *o*-dichlorobenzene solutions at 383 K. See [13].
[30] See for example G. M. Bancroft, and R. H. Platt, Advan. Inorg. Chem. Radiochem. **15**, 59 (1972).
[31] J. N. R. Ruddick, J. R. Sams, and J. Scott, Inorg. Chem. **13**, 1503 (1974).
[32] G. M. Bancroft, V. G. Kumar Das, T. K. Sham and M. G. Clark, J. Chem. Soc., Dalton Trans. **1976**, 643.